Ever J. Barbero[1] *and Edward A. Wen*[1]

Compressive Strength of Production Parts Without Compression Testing

REFERENCE: Barbero, E. J. and Wen, E. A., "**Compressive Strength of Production Parts Without Compression Testing,**" *Composite Structures: Theory and Practice, ASTM STP 1383*, P. Grant, Ed., American Society for Testing and Materials, West Conshohocken, PA, 2000, pp. 470–489.

ABSTRACT: The purpose of this paper is to present a methodology to estimate the compressive strength of fiber-reinforced composite prototype and production parts. The procedure is based on test data that incorporate the effects of sample size and sample preparation but are simpler to obtain than compression test data. A simple formula is derived to relate the compressive strength to the shear stiffness, shear strength, and standard deviation of fiber misalignment. The formula is completely defined in terms of these three parameters, all of which can be measured by standard experimental procedures. It is proposed to use the shear stiffness and shear strength from coupon tests, usually available from the material supplier or from the characterization phase of the design/build project. Since these two parameters are relatively insensitive to part size and sample preparation, the coupon data are reliable and representative of the actual production part. Since fiber misalignment depends on the processing conditions, the third parameter used is the standard deviation of fiber misalignment, measured on samples from actual production parts. These three values characterize the compressive strength of the carbon/epoxy layups for which experimental data are found in the literature and those evaluated in this investigation. The predictions are then validated against data from a variety of specimens tested at high and low temperatures, as well as data from production prototype parts.

KEYWORDS: •••

Nomenclature

C_2	Stress-strain quadratic-term coefficient
Exp	Expected value
F	Cumulative folded probability
f	Folded probability density
F_{1c}	Longitudinal compressive strength
F_6	Composite shear strength
F_{xc}	Off-axis compressive strength of globally misaligned composite
G_{12}	Composite shear stiffness
n	Number of data points
p, q	Parameters in Eq 10
Sv	Standard deviation of sample variance
$t_{\alpha/2,n-1}$	t-distribution at $\alpha/2, n-1$
V	Sample variance
Ω	Standard deviation of fiber misalignment
α	Misalignment angle
α_G	Global misalignment angle
χ	Dimensionless number controlling compression behavior
γ	In-plane shear stress

[1] West Virginia University, Morgantown WV 26506-6106.

σ Bundle stress
σ_{app} Applied stress
σ_{eff} Effective stress
τ In-plane shear stress
ω 1/100 of percentage of buckled fibers

Compressive strength of PMC often controls the design, but yet it is very difficult to measure and very difficult to predict. Various test fixtures give different results (SACMA SRM-1R-94, ASTM D 5379, ASTM D 695, etc.) depending on sample preparation and sample size. Most of these fixtures measure the compressive strength of laboratory samples, which is often higher than that of production parts. But production parts cannot be tested because the specimens would be too thick for those fixtures. When prototype test specimens are tested, other problems such as buckling can mask the results. Additional problems, such as damage, appear when trying to machine samples out of prototype parts.

In the typical "Building Block" development process for large structures [*1*], design allowables are established from specimen tests. Structural elements are then tested to confirm design allowables. Larger elements, or subcomponents, are then tested to reconfirm design allowables and, finally, a full-scale test is performed to prove the entire design. Using the proposed methodology, compressive strength of structural elements can be predicted from available material data (shear stiffness and strength) and easily measured parameters (misalignment), thus reducing the number of structural tests required to substantiate the design process. Also, the proposed methodology can be used to perform failure analysis and postmortem diagnosis of failed composite structures that may be too damaged to be tested in compression.

Many models have been proposed to improve the prediction of compressive strength, the first introduced by Rosen [*2*]. The literature encompasses fiber buckling modes [*3*], kink-band models [*4*], and kink-bands induced by microbuckling [*5*]. In Ref *6*, an analytical formulation was introduced that used the standard deviation of the fiber misalignment to represent the misalignment distribution. An exact solution for microbuckling utilizing a continuum damage model was derived and simplified into an explicit equation for compression strength. In this work, a methodology is developed to predict compressive strength using this explicit equation at the specimen and structural element level.

Materials and Experimental Procedures

Two different carbon/epoxy prepregs were used in this study. The first material, Cytec Fiberite using 949-HYE epoxy and M30GC carbon fibers, has a standard modulus fiber with a tough resin. The second material, Cytec Fiberite using 948A1-HYE epoxy and M40J carbon fibers, has an intermediate modulus fiber and a relatively stiffer matrix.

The prepregs were laid up by hand and cured in an oven at 135°C for 90 min with approximately 27 in. Hg vacuum bag pressure. A 7-ply [0 deg] panel was made for the compression specimens and a 20-ply [0 deg] panel was used for the shear modulus and shear strength specimens. The 7-ply panel was cured with peel ply and caul plates on both sides of the panel so that the surface would have very little waviness and the thickness would be relatively uniform. To achieve low misalignment, great care was taken to align the 7 plies of the prepreg to the manufactured edge of the tape. The 20-ply panel was cured without caul plates or peel ply because the variations in thickness were judged to be small when compared to the total thickness.

Specimen Tests

The SACMA SRM-1R-94 procedure was selected for the longitudinal compression test because it typically provides compressive strengths 5% higher than the ASTM D 3410 "IITRI" method. In addition, the SACMA test would allow easier comparison with manufacturer's data because it is most commonly used by airframe manufacturers, prepreg producers, and so on.

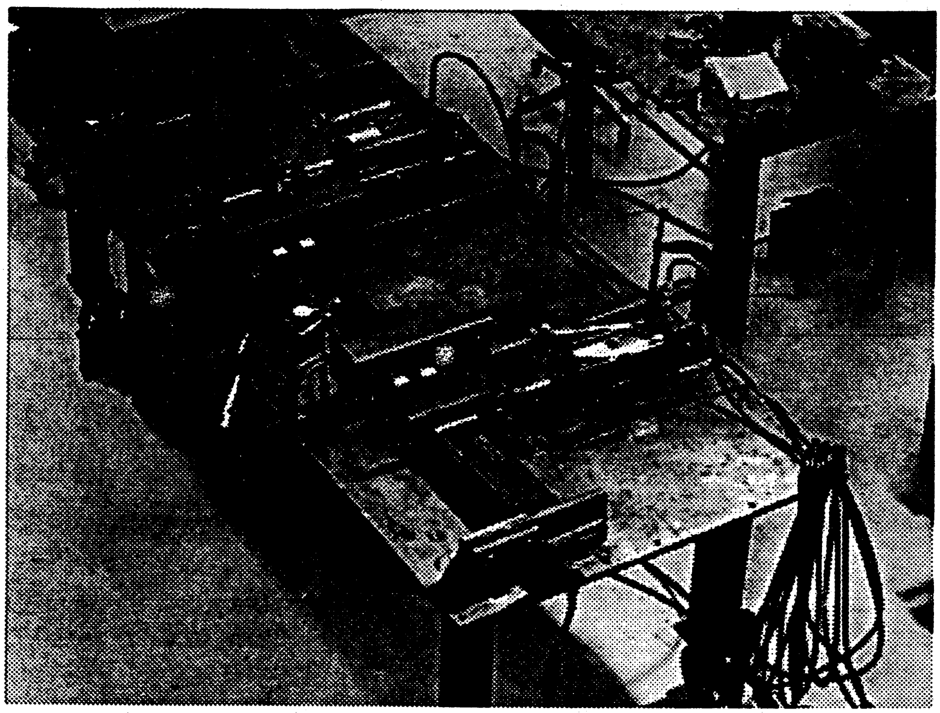

FIG. 1—*Four-point bending test.*

To measure shear strength and modulus, the ASTM D 5379 "Iosipescu" method was selected. MicroMeasurements shear gages were used since they average the shear strain between the entire region between the notches of the specimen. Modulus G_{12} data were taken between 1000 and 6000 microstrains from back-to-back shear gages and the results from each side were averaged together.

The in-plane shear strength, F_6, was taken where there was a significant change in the slope of the load-displacement plot. In the case of the specimens with the tougher resin 949-HYE there was no significant change, so F_6 was taken at the slight dip between the initial curved section and the linear section of the load-displacement plot (see Ref *13*).

The compression, shear strength, and shear modulus tests for the specimens were conducted at 82°C, room-temperature-ambient (RTA) and −87°C for both materials.

Beam Tests

Two C-section beams were tested in four-point bending at room temperature (Fig. 1). These beams were made of 949 HYE/M30GC and were relatively thick hand layups cured at 135°C with 27 in Hg vacuum pressure. In Beam 1, the gage section consisted of 60 ply of 0 deg and one ply ±45 deg on top and bottom. In Beam 2, the gage section had 56 ply with one ±45 deg ply every 8 ply of 0 deg.

Misalignment Characterization

The specimens were cut from panels with a diamond saw and ground to their final dimensions on a surface grinder. After the compression specimens were broken, the two halves of the specimens

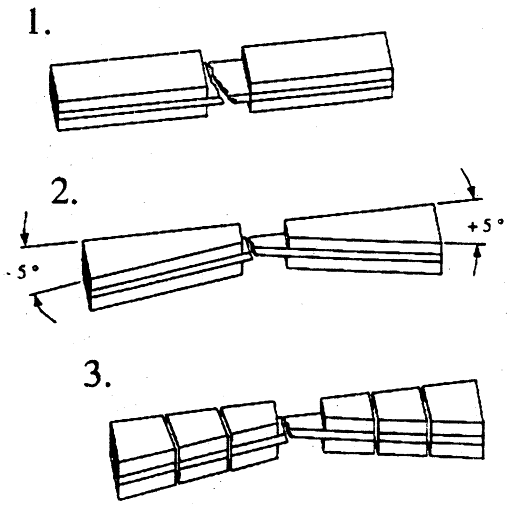

FIG. 2—*Specimen polishing procedure.*

were carefully ground to regain parallel edges. This is possible since the damage from the compression failure is around the gage section and the end of the specimen can still be used to establish a reference surface.

A 5 degree cut was made on each of the compression specimen halves so that one side would have $+5$ deg cut and the other side would have a -5 deg cut (Fig. 2). The specimen was then cut and potted in acrylic with the ± 5 deg surfaces on top. These surfaces were then polished using the Buehler Ecomet 2 Polishing Machine at 240, 400, 600, 800 grit sandpaper and with 1 μm alumina polishing compound.

In the case of the beams, a piece was cut from the compression caps as near as possible to the location of the failure (Fig. 3). A piece cut in this manner had two faces that were against the tool and

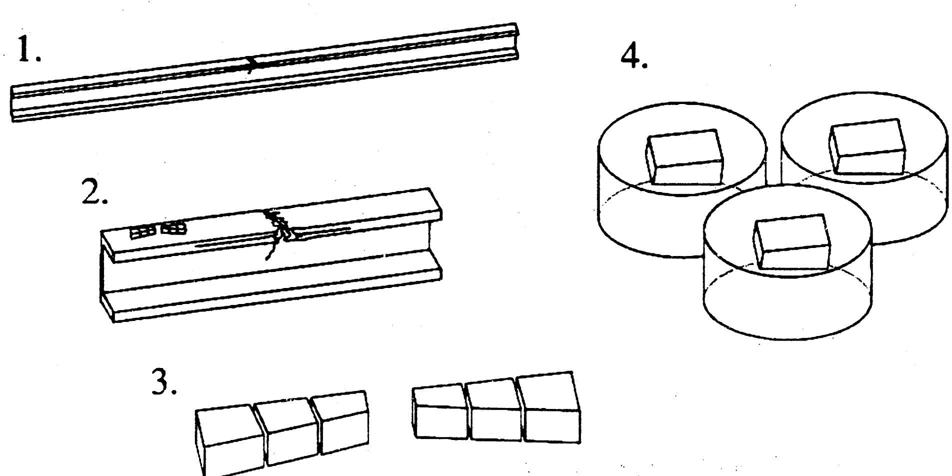

FIG. 3—*Beam sp*

therefore could be taken as reference surfaces when performing the subsequent grinding to square up the specimen. As previously, a +5 deg cut and −5 deg cut were made and then polished until the fibers could be viewed as complete ellipses.

To quantify fiber misalignment, the major and minor axes of the fiber ellipse were measured with a metallographic microscope and a video acquisition software [*13*]. The major axis was measured at ×200 magnification for 1512 fibers on each specimen and the minor axis of the fiber was measured at ×500 magnification for 40 points on each specimen.

As pointed out in Ref *7*, there is a tendency to pick the fibers with a major axis of smaller length and neglect the fibers with a longer length. To make the selection as random as possible, all fibers intersecting a line drawn on the screen were measured (Fig. 4). Data were taken starting from the top of the specimen and ending at the bottom. Additional lines of data were taken until the required number of points had been achieved.

The misalignment angle is computed from the major axis length, the fiber diameter and the angle of the cutting plane [*7,13*]. The distribution is shown to be Gaussian by using the cumulative distri-

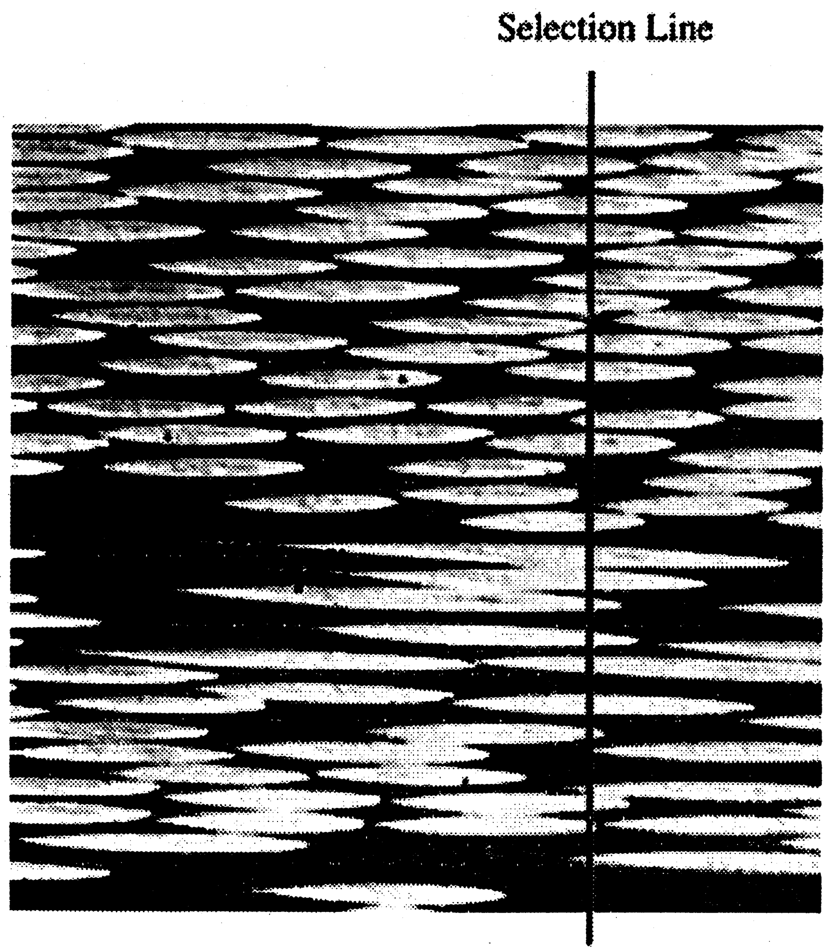

FIG. 4—*Selection of ellipses.*

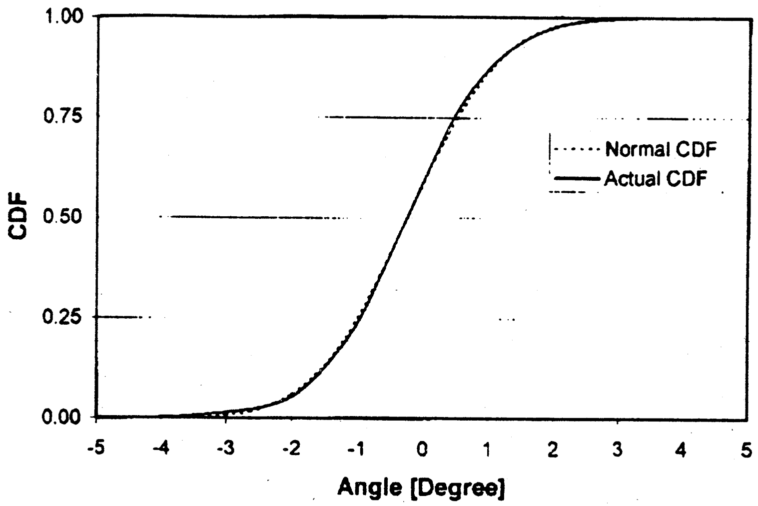

FIG. 5—*Cumulative distribution function of fiber misalignment for a specimen.*

bution function (CDF) in Fig. 5. When the mean of the distribution is zero, all the misalignment data are represented by just one parameter—the standard deviation of fiber misalignment Ω. Otherwise, the mean value is the global misalignment, its effect being considered here in the global misalignment section.

Compressive Strength Formula

The prediction of compression strength of composites was first introduced by Rosen [*2*], assuming that buckling of the fibers initiates a process that leads to the collapse of the material. The effect of initial shear stiffness on the compression strength has been studied experimentally [*8,9*], concluding that higher initial shear stiffness correlates with higher compression strength. The detrimental influence of fiber misalignment has been experimentally demonstrated [*8,10*]. The experimental evidence suggests that fiber buckling of perfectly aligned fibers (Rosen's model) is an imperfection sensitive problem if the shear response of the composite is nonlinear [*16*]. Rosen's model has been refined with the addition of initial fiber misalignment and nonlinear shear stiffness [*3*]. However, most existing models assume that all the fibers have the same value of misalignment α, which is taken as an empirical parameter. Then, the value of this empirical parameter is set so that the model predictions match experimental data. That is, experimental data must be available before the model can be used. Besides, it is well known that there is not a unique value for fiber misalignment for all the fibers but a Gaussian distribution of misalignment (Fig. 5) [*7*].

Although the standard deviation has been used as a single misalignment value in the theoretical models, the predicted compressive strength values did not compare well with experimental data [*12*]. Furthermore, the standard deviation is a measure of the dispersion, not of the expected value of a distribution. From a statistical point of view, a single value of misalignment that in the average represents the population is the expected value, or mean. However, the mean of the misalignment distribution is often equal to zero. Noting that fiber buckling occurs at the same load for positive or negative misalignment angle, the symmetric normal distribution can be converted to a half normal distribution. In the half normal distribution, the random variable is given as $x = \text{abs}\,|\,\alpha\,|$, where α is the random variable of the normal distribution. In other words, the half normal distribution represents the normal distribution without the algebraic sign (negative side gets folded onto the positive side). The expected value of a half normal distribution is

$$\mathrm{Exp} = \int_{x=0}^{x=\infty} \frac{1}{\Omega}\sqrt{\frac{2}{\pi}}\exp\left(\frac{-(x')^2}{2\Omega^2}\right)x'dx' = \sqrt{\frac{2}{\pi}}\,\Omega \tag{1}$$

However, using the expected value of the half-normal distribution as a single misalignment value did not lead to a good correlation with experimental data [*12*]. This means that the process of compression failure cannot be modeled by the mean of the absolute value of misalignment data. Since none of the statistical approaches described above give satisfactory predictions, a different procedure based on a combination of statistics and damage mechanics is introduced next. Basically, it is assumed that the fibers with large misalignment buckle first and the stress is redistributed to the remaining fibers [*11*]. This phenomenon continues until the remaining fibers are no longer capable of sustaining the load, thus defining the compressive strength of the material.

The bundle stress $\sigma(\alpha, \gamma)$ of a fiber bundle with all the fibers having the same misalignment α was derived by Barbero [*6*] following a method similar to Ref *3* and is shown in Fig. 6 for various values of α. For the bundle stress to have a maximum with respect to shear strain γ, a nonlinear shear stress-strain relationship must be used. According to Refs *11*, *13*, and *14*, the equation

$$\tau = F_6 \tanh(G_{12}\gamma/F_6) \tag{2}$$

fits shear experimental data very well. However, a simpler equation

$$\tau = G_{12}\gamma + C_2\gamma^2 \tag{3}$$

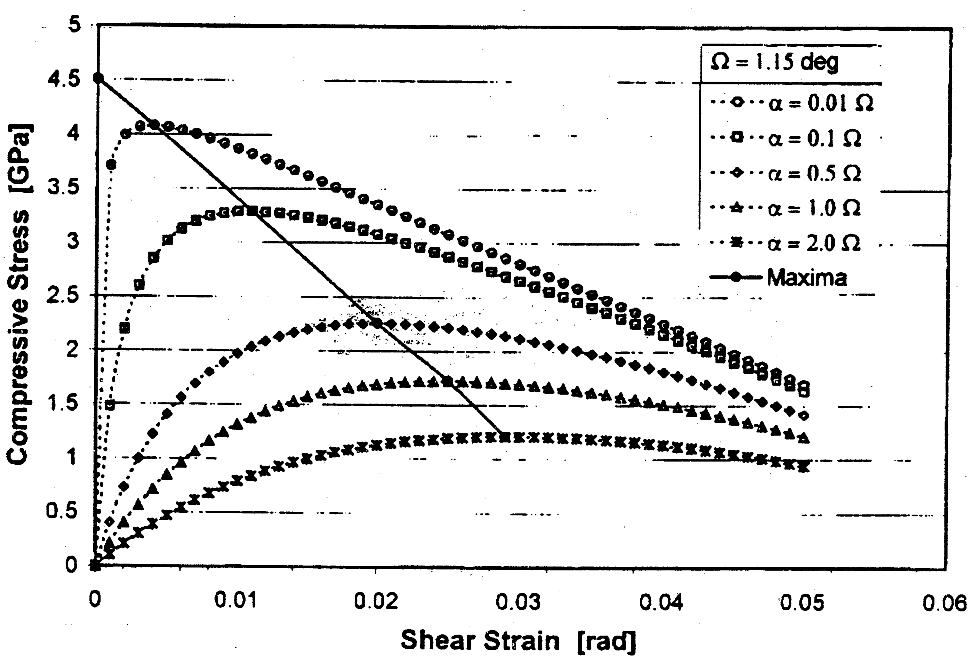

FIG. 6—*Bundle compressive stress vs. shear strain of 949/M30GC.*

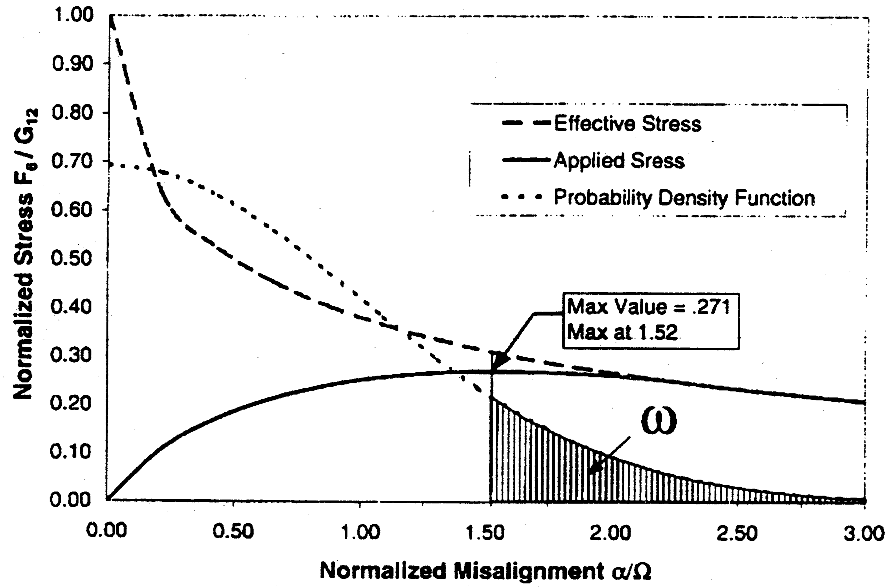

FIG. 7—*Combined buckling/misalignment of 949/M30GC.*

is accurate enough for the prediction of compressive strength provided C_2 is adjusted to fit the data in the interval of shear strain over which compression failure takes place. Taking this interval to be $0 < \gamma < 2F_6/G_{12}$, means that the shear strain will not exceed the point where the secant shear modulus is ½ of the original one. Most composites, including carbon-epoxy and glass-polyester, will fail in compression within this range. Then, the constant C_2 is found in terms of the parameters in Eq 2, taking into account that $\tanh(2) \approx 1$, as

$$C_2 = -\frac{G_{12}^2}{4F_6} \tag{4}$$

Following the procedure in Ref *6* but using Eq 3 instead of Eq 2, the bundle stress is obtained as

$$\sigma(\alpha, \gamma) = \frac{\gamma G_{12}}{\gamma + \alpha} + \frac{8}{3}\frac{C_2\gamma^2}{3(\gamma + \alpha)\pi} \tag{5}$$

The axial-stress versus shear-strain plot has a maximum for each misalignment value α, as shown in Fig. 6. The loci of maxima represent the bundle strength $\sigma_{\text{eff}}(\alpha)$ of a fiber bundle of a composite with all fibers equally misaligned at angle α, and it is shown by a dashed line in Fig. 7. Since such a composite does not exist, the Gaussian distribution of fiber misalignment must be brought in.

Continuous damage mechanics (CDM) was used [*6*] to combine the Gaussian distribution of misalignment with Eq 5. The misalignment distribution is Gaussian, and its probability density is given by

$$f(\alpha) = \frac{1}{\Omega\sqrt{2\pi}}\, e\left(\frac{-\alpha^2}{2\Omega^2}\right), \quad -\infty < \alpha < \infty \tag{6}$$

where Ω is the standard deviation of fiber misalignment. Therefore, the area fraction of composite that has fiber misalignment in excess of abs $|\alpha|$ is given by

$$\omega = \int_{\alpha}^{\infty} \frac{1}{\Omega}\sqrt{\frac{2}{\pi}}\exp\left(\frac{-(x')^2}{2\Omega^2}\right)x'dx' \quad ; \quad 0 \le \omega \le 1 \tag{7}$$

which corresponds to the shaded area under the folded probability density of fiber misalignment in Fig. 7. The folded distribution, $f(\text{abs}\,|\alpha|)$, is used because fiber microbuckling is indifferent to the sign of the misalignment. Since the integral above is transcendental, it is approximated by

$$F(\alpha) = 0.8341342\frac{\alpha}{\Omega} - 0.1727790\left(\frac{\alpha}{\Omega}\right)^2 \tag{8}$$

For a given value of applied stress σ_{app}, a number of fibers buckle because they have sufficiently high misalignment. The load is carried by the unbuckled fibers, having area $(1 - \omega)$. Therefore the applied stress is

$$\sigma_{app} = \sigma_{eff}(\alpha)[1 - \omega(\alpha)] \tag{9}$$

which is shown as a solid line in Fig. 7. The maximum of the applied stress is the compressive strength, given by

$$F_{1c} = G_{12}\left(\frac{\chi}{p} + 1\right)^q, p = 0.21, q = -0.69 \tag{10}$$

in terms of the dimensionless number

$$\chi = \frac{G_{12}\Omega}{F_6} \tag{11}$$

Equation 10 does not contain empirically adjustable factors and is simple enough to be used in practice. The parameters p and q are not set to fit any empirical data; they are obtained as the result of finding the maximum of Eq 9 using the procedure described in Ref *6*. It will be shown that predictions using Eq 10 compare well with compression strength data for a broad class of materials.

Statistical Analysis

Given that previous studies [*12*] used 1000 points of data for carbon fiber prepregs, 1512 points were taken for each specimen to provide a comfortable margin of accuracy. As many as 756 points of data were taken on the +5 deg side of the specimen and the same number on the −5 deg side.

Considering only one side of the specimen, the misalignment distributions are slightly skewed from a perfectly normal distribution because of a bias in the measurement technique [*13*]. For example, the +5 deg side (right side) usually has a distribution with more negative angles and therefore a negative skew (Fig. 8), while the −5 deg side has the opposite. In almost all of the cases, the fiber angles were between ±5 deg. If there were some points outside ±5 deg, these were discarded since they do not make a strong contribution to the compression strength of the laminate [*12*].

As discussed earlier, it is reasonable to expect that the distribution is normal and therefore the bias is attributed to the measurement technique. To cancel the bias, it is proposed to use the data from the

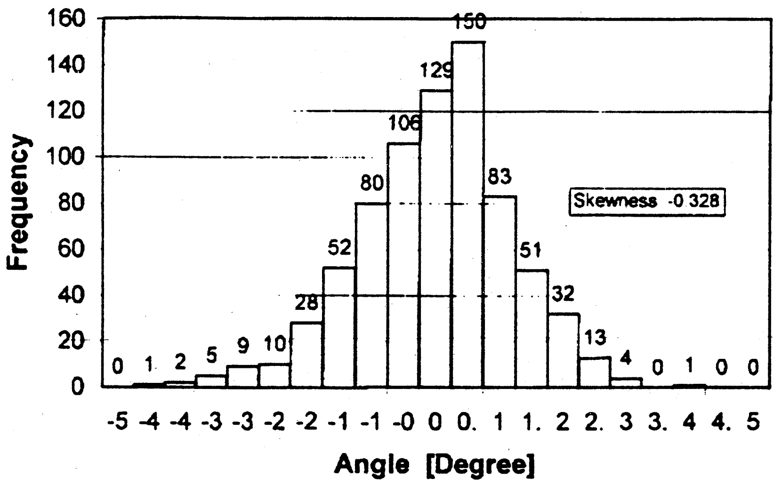

FIG. 8—*Distribution skew example. Sample NTP-15-86 right side angles.*

+5 and the −5 deg sides of the specimen and combine them together. The mean angle is shifted to zero before combining the results from both sides. This is reasonable because the average angle before shifting to zero was usually much less than ±0.5 deg, which is within ±0.5 deg tolerance due to cutting and polishing of the specimen. Once the plus and minus side data are combined, the data are normal (Gaussian) with negligible skew as shown in Fig. 5.

Standard deviation Ω was obtained from four 949 HYE/M30GC SACMA specimens, four 948A1 HYE/M40J SACMA specimens, four samples from beam 1 and four samples from beam 2. Confidence intervals at the 95% confidence level were constructed for each set using $n = 4$ and the t-distribution as given below

$$\sqrt{V - \frac{t_{\alpha/2,n-1}S_V}{\sqrt{n}}} \leq \Omega \leq \sqrt{V + \frac{t_{\alpha/2,n-1}S_V}{\sqrt{n}}} \tag{12}$$

where

Ω = population standard deviation
V = sample variance
S_v = standard deviation of sample variance
α = probability
n = number of data points
$t_{\alpha/2,n-1}$ = t-distribution at $\alpha/2$, $n - 1$.

The results are summarized in Table 1 and 2. Since a very large number of fibers (1512) were used in the computation of each of the four Ω values, these can be considered to be exact, with very narrow individual confidence intervals, computed using the χ^2 distribution (Tables 1, 2).

The t-distribution was also used to establish the confidence intervals for the actual compression strengths, shear strengths, and shear moduli at the three test temperatures. Again, the confidence interval is at the 95% confidence level (Tables 3, 4).

TABLE 1—*949/M30GC confidence intervals on* Ω.

Type of Sample	I.D.	Specimen Standard Deviation, $n = 1512$ [deg]	95% Confidence Interval, (χ^2 dist.) [deg]	Population Standard Deviation Ω, $n = 4$ [deg]	95% Confidence Interval (t - dist). [deg]
949/M30GC SACMA compression specimen	NTP-15-1	1.236	+0.046 −0.043		
	NTP-15-84	1.123	+0.042 −0.039	1.150	+0.091 −0.099
	NTP-15-86	1.129	+0.042 −0.039		
	NTP-15-21	1.109	+0.041 −0.038		
949/M30GC Beam 1	B1-1	1.342	+0.0500 −0.046		
	B1-L1R1	1.328	+0.049 −0.046	1.313	+0.091 −0.097
	B1-L2R2	1.223	+0.045 −0.042		
	B1-L3R3	1.355	+0.050 −0.047		
949/M30GC Beam 2	B2-1	1.158	+0.043 −0.040		
	B2-L1R1	1.134	+0.042 −0.039	1.125	+0.055 −0.058
	B2-L2R2	1.074	+0.040 −0.370		
	B2-L3R3	1.133	+0.042 −0.039		

Predicted Results

Although Eq 10 predicts the experimental data from Refs *11* and *12* very well (Fig. 9), confidence intervals were not available in the literature to truly evaluate the merits of the proposed methodology. In this project, confidence intervals on the predicted compressive strength were obtained from the experimental confidence intervals on the parameters involved, namely G_{12}, F_6, and Ω. Values of the parameters and their experimental confidence intervals are shown in Tables 1 to 4. Those confidence intervals were obtained using the t-distribution (Eq 12) and the experimentally obtained sample variance from testing.

Because the three terms in the compression Eq 10 all have their own confidence interval, the predicted compression strength will have its associated confidence interval. By substitution in Eq 10, it can be shown that the highest value of F_{1C} occurs when G_{12} and F_6 are at their highest value and Ω is at its lowest. The lowest values of F_{1C} occur when the values take the opposite extremes, which is consistent with intuition.

Actual versus predicted compressive strengths of the SACMA specimens and four-point beam bending specimens are shown in Figs. 10 to 12. The formula predicts the compressive strength of the RTA and −87°C compression specimens very well. However, the 82°C specimen strength predictions were low even when using the full extent of the confidence interval. This is believed to be partly caused by the large changes in shear modulus that occur at high temperature. It can be inferred from

TABLE 2—*948A1/M40J confidence intervals on* Ω.

Type of Sample	I.D.	Specimen Standard Deviation, n = 1512 [deg]	95% Confidence Interval, (χ^2 dist.) [deg]	Population Standard Deviation Ω, n = 4 [deg]	95% Confidence Interval, (t - dist). [deg]
948A1/M40J SACMA Compression Specimen	NTP-11-1	1.129	+0.040 −0.039	1.205	+0.157 −0.181
	NTP-17-7	1.164	+0.041 −0.040		
	NTP-16-5	1.163	+0.041 −0.040		
	NTP-11-21	1.352	+0.048 −0.047		

TABLE 3—*949/M30GC confidence intervals on* G_{12}, F_6, *Actual* F_{1C}.

Material	Temp. (C)	G_{12} (GPa)	95% Confidence Interval (*t*-dist.) (GPa)	F_6 (MPa)	95% Confidence Interval (*t*-dist.) (MPa)	F_{1c} Actual (GPa)	95% Confidence Interval (*t*-dist.) (GPa)
949/M30GC	82.2	2.86	+0.204	47.5	+3.21	1.03	+0.37
			−0.204		−3.21		−0.037
	23.0	4.51	+0.204	76.7	+4.86	+1.28	+0.148
			−0.204		−4.86		−0.148
	−87.2	4.91	+0.157	125.3	+7.09	+1.56	+0.080
			−0.157		−7.09		−0.080

948 A1/M40J

TABLE 4—*948/M40J confidence intervals on* G_{12}, F_6, *actual* F_{1C}.

Material	Temp. (C)	G_{12} (GPa)	95% Confidence Interval (*t*-dist.) (GPa)	F_6 (MPa)	95% Confidence Interval (*t*-dist.) (MPa)	F_{1c} Actual (GPa)	95% Confidence Interval (*t*-dist.) (GPa)
948A1/M40J	82.2	3.46	+0.268	70.3	+0.976	1.34	+0.094
			−0.268		−0.976		−0.094
	23.0	4.92	+0.094	89.8	+1.76	1.43	+0.039
			−0.094		−1.76		−0.039
	−87.2	5.32	+0.307	112.6	+8.03	1.54	+0.128
			−0.307		−8.03		−0.128

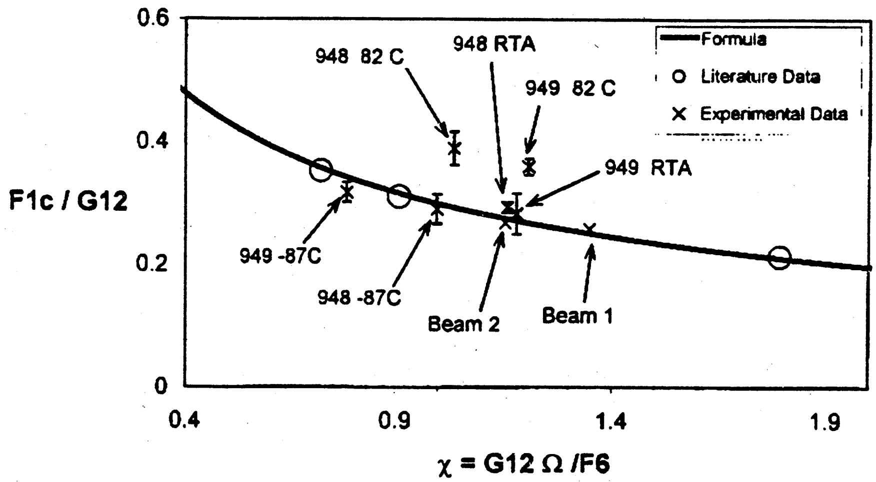

FIG. 9—*Formula vs. experimental data. Literature data from Refs* 11 *and* 12.

Tables 3 and 4 that shear strength is almost linear in the −87°C to 82°C temperature range while shear modulus has a large decrease between RTA and 82°C. Residual stresses may also play a role in the discrepancy.

Global Misalignment

When a layup has global misalignment α_G, but the misalignment of various layers is balanced and symmetric $[\pm\alpha_G]_s$, the laminate compressive strength can be found by stress transformation [*14*, p. 200]

$$F_{XC} = F_{1c}\cos^2(\alpha_G) \tag{13}$$

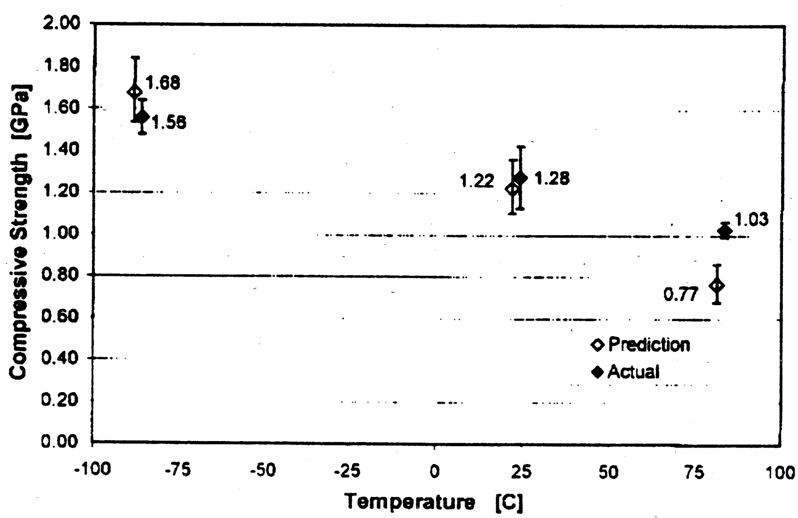

FIG. 10—*949/M30GC SACMA predicted vs. actual* F_{1c}.

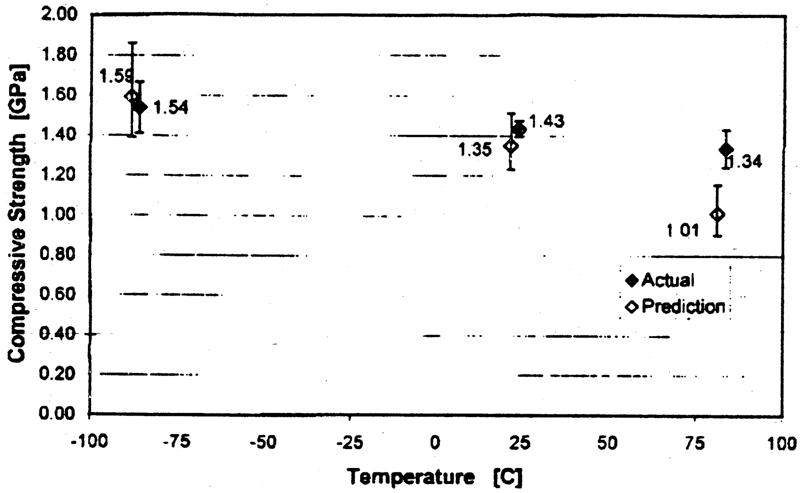

FIG. 11—*948A1/M40J SACMA predicted vs. actual* F_{1c}.

Using data from Ref *15*, it was found in this investigation that Eq 13 provides good agreement in the range $0 < \alpha_G < 10$ deg. However, there exists no known method for estimating the strength of laminates with unbalanced, global misalignment $[+\alpha_G]_n$ or $[-\alpha_G]_n$.

When there is unbalanced global misalignment, the equilibrium Eq 5 still applies but the distribution of fiber angles is shifted by the average angle α_G to

$$f(\alpha, \alpha_G) = \frac{1}{\Omega\sqrt{2\pi}} e^{\left(\frac{-(\alpha - \alpha_G)^2}{2\Omega^2}\right)}, \quad -\infty < \alpha > \infty \tag{14}$$

$-\infty < \alpha < \infty$

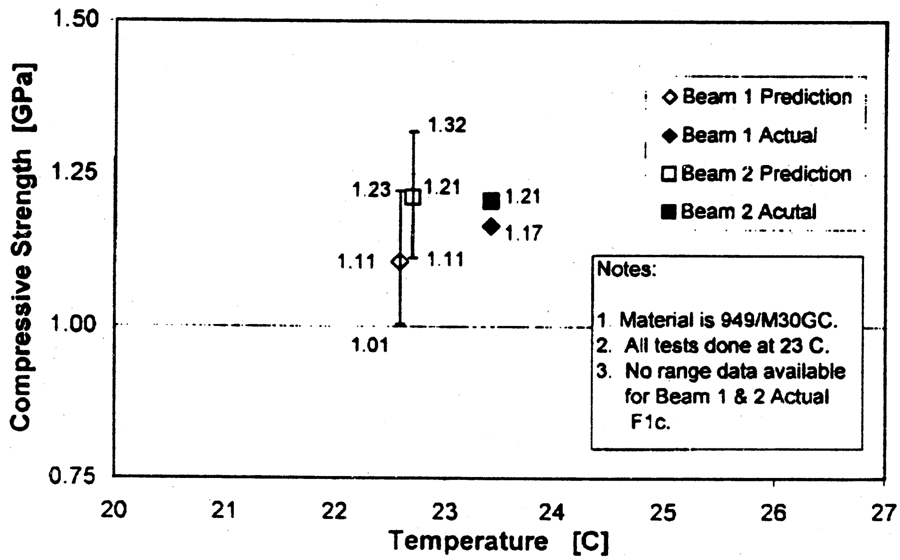

FIG. 12—*949/M30GC Beam 1 and 2 predicted vs. actual* F_{1c}.

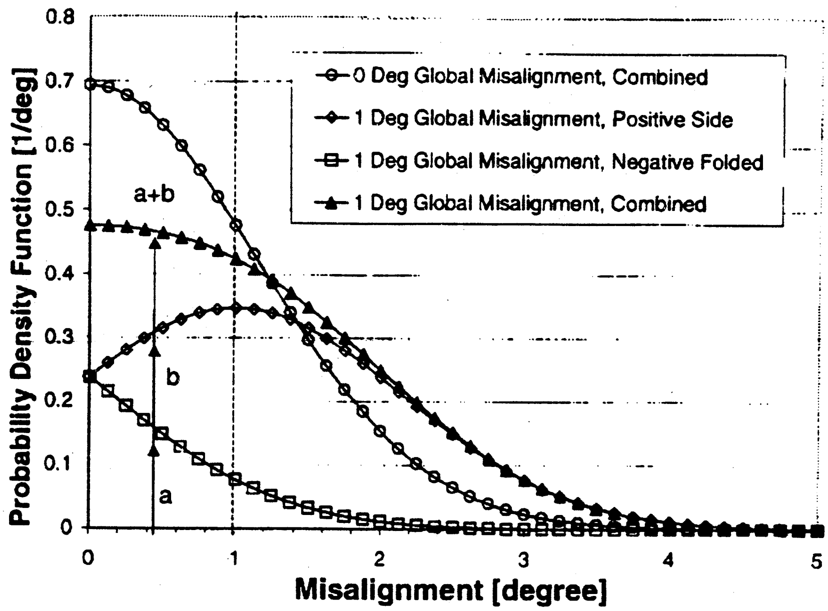

FIG. 13—*Shifted probability density function at 0, 1.0 global misalignment.*

The area fraction of composite with misalignment in excess of abs $|\alpha|$ is no longer given by Eq 5 because there is no symmetry about zero. Therefore, the quadratic polynomial approximation (Eq 8) cannot be used. Instead of using Eq 7, the integral

$$\omega = F(\alpha) = 2\int_{\alpha}^{\infty} f(\alpha', \alpha_G)d\alpha' \quad ; \quad 0 \leq \omega \leq 1 \tag{15}$$

must be integrated numerically. To illustrate the integration, the case of 1.0 degree global misalignment is shown in Fig. 13. The function is folded about zero and the two distributions are added together. For comparison, the probability density function for 0 deg global misalignment is shown also.

The integration of the combined shifted probability density used to obtain the cumulative distribution function at the given angles of global misalignment is shown in Fig. 14. When multiplied by the effective stress (dashed line in Fig. 7), the resulting applied stress curves are similar to the solid line in Fig. 7 [*13*]. The maximum of each curve represents the compressive strength at the given global misalignment angle. This technique is informally called the "Method of Shifted Distributions."

Note that Figs. 13 and 14 are for a fixed value of $\Omega = 1.15$ degrees. If taken at different values, it would produce a family of curves for F_{1C} as a function of Ω and α_G [*13*]. In this way, Fig. 15 was constructed to show the compressive strength F_{1C} as a function of global misalignment α_G when the standard deviation of fiber misalignment is fixed at various values. An individual curve represents a part fabricated with a prepreg layup that has a given value of Ω and is oriented with a global misalignment α_G with respect to the nominal direction (load direction).

Finally, it should be pointed out that laminate compressive strength is often controlled by the unidirectional layers [*15,17*]. Therefore, the proposed methodology applies not only to unidirectional composites but to laminated composites as well.

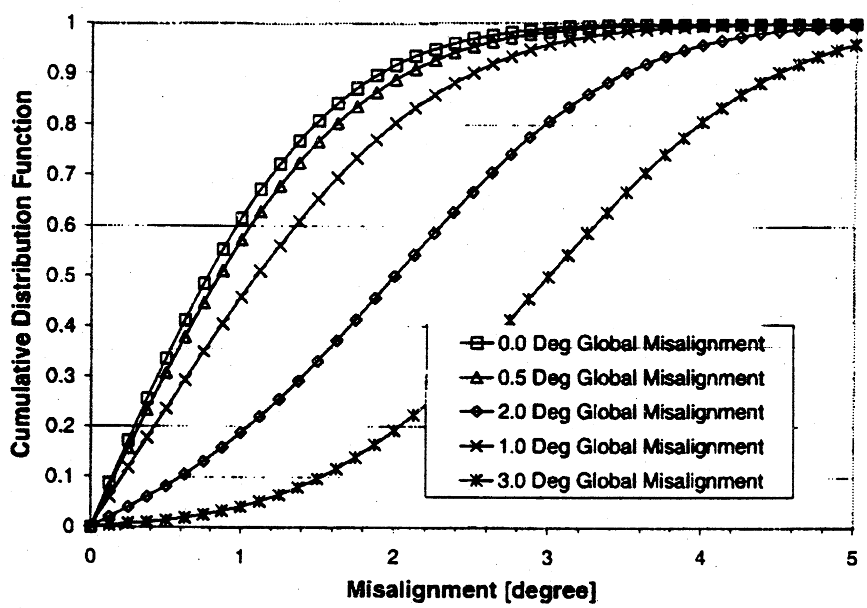

FIG. 14—*Cumulative distribution functions of the shifted probability density.*

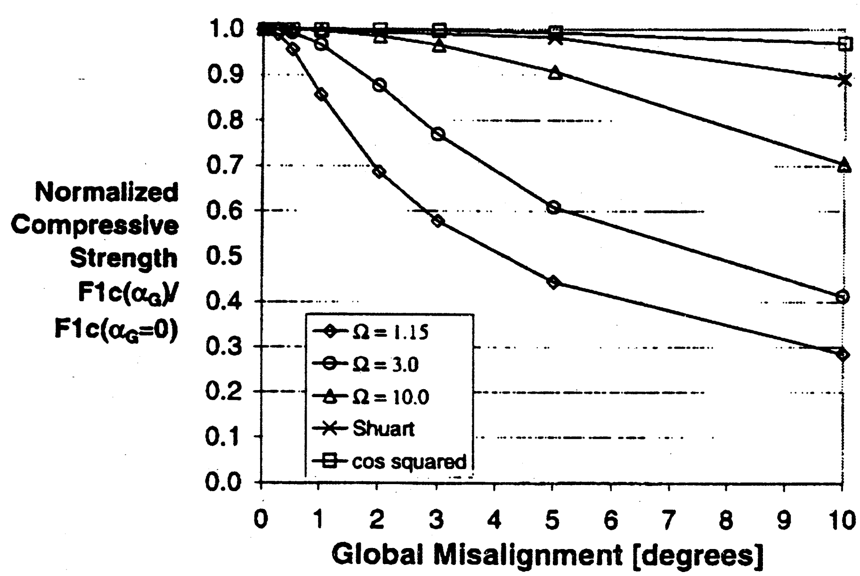

FIG. 15—*Normalized* F_{1c} *vs. global misalignment.*

Summary

The proposed methodology consists of the following:

a. Measure the global misalignment angle α_G and the standard deviation of fiber misalignment Ω on the actual part. This may be done on witness coupons or on the part itself during postmortem diagnosis.
b. Use the shear stiffness G_{12} and shear strength F_6 values from coupon data. Since these values are quite insensitive to sample size and preparation, they should be representative of the actual part. If in doubt, cut and test ASTM D 5379 coupons from the part itself.
c. Estimate the compressive strength of the material using Eq 10 in terms of the dimensionless number χ defined in Eq 11.
d. If the global misalignment is different from zero, use the procedure described in the foregoing global misalignment section to estimate the off-axis compressive strength.

Conclusions

When fiber misalignment data are combined with the shear stiffness and strength data of the material, the prediction formula presented in this paper accurately predicts the compressive strength of SACMA SRM-1R-94 compression specimens and beams in four-point bending at room temperature and at $-87°C$. At 82°C, the prediction is conservative by a 25% margin. It is clear that the proposed methodology can predict accurately the values of compressive strength, thus reducing the need for compression testing to substantiate the design process. In addition, this technique has application to "postmortem" analysis, where misalignment measurement on the failed structure combined with material shear data can be used to accurately estimate the compressive strength without compression testing. The technique proposed to predict compressive strength with global misalignment $[+\alpha_G]_n$ or $[-\alpha_G]_n$ also holds promise. From an experimental point of view, a procedure was presented to eliminate the skewness of the optical procedure used to measure fiber misalignment. Future work would include devising a means to verify the global misalignment predictions and to incorporate the effect of voids into the compressive strength model.

Acknowledgment

This project was partially sponsored by Aurora Flight Sciences under contract AWV97-2348. Our thanks go to Les Montford, Randy Tatman, Clint Church, and Alistar Wroe for providing the prototype data and guidance for the study.

References

[1] Dobyns, A., "RAH-66 Comanche Building Block Structural Qualification Program," ASTM Symposium on Composite Structures: Theory and Practice, *ASTM STP 1383*, 17–18 May 1999, Seattle, WA.
[2] Rosen, B. W., Chapter 3 in "Fiber Composite Materials," Metals Park, OH, American Society for Metals, 1965.
[3] Wang, A. S. D., "A Non-Linear Microbuckling Model Predicting the Compressive Strength of Unidirectional Composites," ASME Winter Annual Meeting, ASME Paper 78-WA/Aero-I, 1978.
[4] Lagoudas, D. C. and Saleh, A. M., "Compressive Failure Due to Kinking of Fibrous Composites," *Journal of Composite Materials*," Vol. 27, 1993, pp. 83–106.
[5] Yin, W.-L., "A New Theory of Kink Band Formation," AIAA-92-2552-CP, 1992.
[6] Barbero, E. J., "Prediction of Compression Strength of Unidirectional Polymer Matrix Composites," *Journal of Composite Materials*, Vol. 32, No. 5, 1998, pp. 483–502.
[7] Yurgartis, S. W., "Measurement of Small Angle Fiber Misalignment in Continuous Fiber Composites," *Composite Science and Technology*, Vol. 30, 1987, pp. 279–293.
[8] Yurgartis, S. W. and Sternstein, S. S., "Experiments to Reveal the Role of Matrix Properties and Composite Microstructure in Longitudinal Compression Strength," ASTM Symposium on Compression Response of Composite Structures, 16–17 November 1992.

[9] Crasto, A. S. and Kim, R. Y., "The Effects of Constituent Properties on the Compression Strength of Advanced Composites," ASTM Symposium on Compression Response of Composite Structures. 16–17 November 1992.

[10] Mrse, A. and Piggott, "Relation between Fibre Divagation and Compressive Properties of Fibre Composites," *Proceedings 35th International SAMPE Symposium*, 2–5 April 1990, pp. 2236–2244.

[11] Barbero, E. J. and Tomblin, J. S., "A Damage Mechanics Model for Compression Strength of Composites," *International Journal of Solid Structures*, Vol. 33, No. 29, 1996, pp. 4379–4393.

[12] Haberle, J. G., "Strength and Failure Mechanisms of Unidirectional Carbon Fibre-Reinforced Plastics Under Axial Compression," Ph.D. thesis, Imperial College, London, U.K., 1991.

[13] Wen, E., "Compressive Strength Prediction for Composite Unmanned Aerial Vehicles," thesis, West Virginia University, Morgantown, WV, 1999.

[14] Barbero, E. J., "Introduction to Composite Materials Design," Taylor and Francis, Philadelphia, PA, 1999.

[15] Shuart, M. J., "Failure of Compression-Loaded Multidirectional Composite Laminates," *AIAA Journal*, Vol. 27, 1989, pp. 1274–1279.

[16] Tomblin, J. S., Barbero, E. J., and Godoy, L. A., "Imperfection Sensitivity of Fiber Micro-Buckling in Elastic-Nonlinear Polymer-Matrix Composites," *International Journal of Solid Structures*, Vol. 34, No. 13, 1997, pp. 1667–1679.

[17] Barbero, E. J., Makkapati, S., and Tomblin, J. S., "Experimental Determination of Compressive Strength of Pultruded Structural Shapes," *Composite Science and Technology*, Vol. 59, 1999, pp. 2047–2054.